

# **Quantifying the missing link between forest albedo and productivity in the boreal zone**

Aarne Hovi<sup>1</sup>, Jingjing Liang<sup>2</sup>, Lauri Korhonen<sup>3</sup>, Hideki Kobayashi<sup>4</sup>, Miina Rautiainen<sup>1,5</sup>

<sup>1</sup>Department of Built Environment, School of Engineering, Aalto University, P.O.Box 15800, 00076 AALTO, Finland

<sup>2</sup>School of Natural Resources, West Virginia University, P.O.Box 6125, Morgantown, WV 26505, USA

<sup>3</sup>School of Forest Sciences, University of Eastern Finland, P.O.Box 111, 80101 Joensuu, Finland

<sup>4</sup>Department of Environmental Geochemical Cycle Research, Japan Agency for Marine-Earth Science and Technology, 3173-25, Showa-machi, Kanazawa-ku, Yokohama, 236-0001, Japan

<sup>5</sup>Department of Radio Science and Engineering, School of Electrical Engineering, Aalto University, P.O. Box 13 000, 00076 AALTO, Finland

*Correspondence to:* Aarne Hovi (aarne.hovi@aalto.fi)

**Abstract.** Albedo and fraction of absorbed photosynthetically active radiation (FAPAR) determine the shortwave radiation balance and productivity of forests. Currently, the physical link between forest albedo and productivity is poorly understood, yet it is crucial for designing optimal forest management strategies for mitigating climate change. We investigated the relationships between boreal forest structure, albedo and FAPAR using radiative transfer model FRT and extensive forest inventory data sets ranging from southern boreal forests to the northern tree line in Finland and Alaska (N = 1086 plots). The forests in the study areas vary widely in structure, species composition, and human interference, from intensively managed in Finland to natural growth in Alaska. We show that FAPAR of tree canopies (FAPAR<sub>CAN</sub>) and albedo are tightly linked in boreal coniferous forests, but the relationship is weaker if the forest has broadleaved admixture, or if canopies have low leaf area and the composition of forest floor varies. Furthermore, the functional shape of the relationship between albedo and FAPAR<sub>CAN</sub> depends on the angular distribution of incoming solar irradiance. We also show that forest floor can contribute to over 50% of albedo or total ecosystem FAPAR. Based on our simulations, forest albedos can vary notably across the biome. Because of larger proportion of broadleaved trees, the studied plots in Alaska had higher albedo (0.141–0.184) than those in Finland (0.136–0.171) even though the albedo of pure coniferous forests was lower in Alaska. Our results reveal that variation in solar angle will need to be accounted for when evaluating climate effects of forest management in different latitudes. Furthermore, increasing the proportion of broadleaved trees in coniferous forests is the most important means of maximizing albedo without compromising productivity: based on our findings the potential of controlling forest density (i.e., basal area) to increase albedo may be limited compared to the effect of favoring broadleaved species.

**Keywords:** FAPAR, conifer, broadleaved, radiative transfer, basal area, leaf area index, AGB, thinning

## 34 1 Introduction

35 Forest management practices, such as thinning and logging, alter the spatial, structural, and species composition of forests.  
36 Through an altered albedo and productivity, these management practices may cause profound impacts on climate. Because  
37 forest structure and species composition influence albedo, managing forests to increase albedo is a potential means of  
38 maximizing the climate cooling effects of forests (Bright et al., 2014; Alkama & Cescatti, 2016; Naudts et al., 2016).  
39 However, if forest management practices are altered in order to maximize albedo, productivity may be compromised, which  
40 would result in reduced carbon uptake as well as reduced timber production and corresponding economic losses. There is an  
41 urgent need to understand how forest management practices change forest albedo, and how forest albedo and productivity  
42 are interconnected.

43

44 Being the world's largest land-based biome, the boreal forest zone consists of vast forest areas under various human  
45 interference levels, from natural growth to intense silvicultural management. The biome plays an important role in  
46 controlling the global carbon and energy balances. It is estimated that the boreal forests comprise 32% of the total carbon in  
47 the world's forests, and account for a significant portion of the carbon uptake (Pan et al., 2011). In addition, the albedo of  
48 boreal forests varies considerably by forest structure, phenology, and snow cover (e.g., Ni & Woodcock, 2000; Kuusinen et  
49 al., 2012; Bright et al., 2013; Kuusinen et al., 2016).

50

51 Previous studies based on local in situ measurements, or remote sensing data for local to regional study areas have shown  
52 that boreal forest albedo is influenced by tree species, with broadleaved species rendering higher albedos than coniferous  
53 (Lukeš et al., 2013a, Kuusinen et al., 2014). Albedo of open areas or that of the forest floor is usually higher than in the  
54 canopy areas (Bright et al., 2014, Kuusinen et al., 2014), except for burned sites (Amiro et al., 2006). A declining trend in  
55 albedo with forest height or age has been observed for coniferous forests (Amiro et al., 2006; Kirschbaum et al., 2011; Bright  
56 et al., 2013; Kuusinen et al., 2016) and may be at least partly explained by the increasing leaf area index (LAI) and thus  
57 reduced contribution of the forest floor on albedo as the forests mature. Similarly, a declining trend in albedo with canopy  
58 density has been observed (Lukeš et al., 2013a).

59

60 Gross primary productivity of vegetation can be approximated by FAPAR, i.e. the fraction of PAR radiation (400–700 nm)  
61 absorbed by the vegetation canopy (Gobron & Verstraete, 2009), because photosynthesis is ultimately driven by the  
62 available solar energy. FAPAR is useful in monitoring and comparing productivity both spatially and temporally, especially  
63 in the absence of accurate growth and yield models, although it should be noted that productivity is affected also by light use  
64 efficiency (LUE) i.e. the efficiency by which plants convert the solar energy into photosynthesis products (Monteith, 1972).  
65 The main determinants of forest canopy FAPAR are leaf area index (LAI) and the directionality of incoming solar radiation  
66 (Majasalmi et al., 2014), because they determine the fraction of PAR radiation interceptable by the canopy. Similarly to

67 albedo, boreal forest FAPAR may differ by tree species (Roujean et al., 1999; Steinberg et al., 2006; Chasmer et al., 2008;  
68 Serbin et al., 2013; Majasalmi et al., 2015) and stand age (Serbin et al., 2013), as both species and age are likely to influence  
69 the LAI of the canopy.

70

71 Estimation methods set limits for the information that can be obtained on the spatial and temporal variation of albedo and  
72 FAPAR. In situ measurements are accurate and can be directly linked with field measured forest structure. On the other  
73 hand, they are extremely tedious and cannot cover large variations in forest structure. Satellite data provide ample coverage  
74 of varying forest structures and wide spatial extent but may compromise spatial resolution and detail in the characterization  
75 of forest structure. In addition, neither local albedo measurements nor satellite-based albedo products can explain the  
76 causality between small-scale environmental management scenarios and changes in albedo or FAPAR. Radiative transfer  
77 models offer a solution to these problems: forest radiative transfer models are a powerful tool for linking quantitative  
78 changes in vegetation structure to albedo or FAPAR for large geographical regions. The models are parameterized using  
79 mathematical descriptions of canopy structure (e.g., LAI, tree height, crown dimensions, stand density), optical properties of  
80 foliage and forest floor, and spectral and angular properties of incoming radiation. Using these models, the albedo and  
81 FAPAR of a forest can be calculated from readily measurable variables such as forest structure and leaf optical properties.

82

83 To our knowledge only one study has examined the relation between forest albedo and FAPAR (Lukeš et al., 2016). In that  
84 study, coarse resolution satellite products (MODIS) were used and one geographical area (Finland) was studied.  
85 Furthermore, previous studies on forest structure and albedo have mainly focused on local geographical scales (e.g. Finland,  
86 Norway, but see Kuusinen et al. (2013) for comparison between Finland and Canada). Comparison of the relationships  
87 between forest structure, albedo and FAPAR has not been performed across the biome, i.e. including both European and  
88 North American boreal forests which have very different natural structures and forest management scenarios. Due to the  
89 large north-south gradient and consequent structural diversity of forests in the boreal zone, the impact of forest management  
90 on albedo cannot be expected to be the same.

91

92 Here we report results from quantifying the links between boreal forest structure, albedo and FAPAR ranging from southern  
93 boreal forests to the northern tree line using detailed, large forest inventory data sets from Finland and Alaska (N = 1086  
94 plots). The forests in the study areas vary widely in structure, species composition, and human interference, from intensively  
95 managed (regularly thinned) forests in Finland to natural growth in Alaska. Using a radiative transfer modeling approach, we  
96 quantify the effects of forest structure and species composition on albedo and FAPAR in order to answer how forest  
97 management practices can be optimized for climate change mitigation. The significant benefit of the modeling approach is  
98 that it enables to study structurally varying forests over large geographical areas, without compromising detail in the forest  
99 structure representation or in the spatial resolution. Our study is therefore the first intercontinental study connecting albedo  
100 and productivity of boreal forests, using accurate ground reference data.

## 101 2 Materials and methods

### 102 2.1 Study areas and field plots

103 This study is based on 1086 field plots located in Alaska, USA, and in Finland, between Northern latitudes of 60° and 68°.  
104 At these latitudes, solar zenith angle (SZA) at solar noon at midsummer ranges from 37° to 45°, and the annual average from  
105 69° to 72°.

106

107 The field plots in Alaska (N = 584) were permanent sample plots established as part of Co-operative Alaska Forest Inventory  
108 that aims at long-term monitoring of forest conditions and dynamics (Malone et al., 2009). The plots were scattered in  
109 interior and southcentral Alaska across a region of about 300 000 km<sup>2</sup>, from Fairbanks in the north to the Kenai Peninsula in  
110 the south (Fig. 1, for more details see Liang et al. (2015)). Some of the plots were measured more than once. We used only  
111 the most recent measurement of each plot. The plots in Finland (N = 502) were temporary or permanent sample plots. They  
112 were located at four separate sites: Hyytiälä (Majasalmi et al., 2015), Koli, Sodankylä, and Suonenjoki (Korhonen, 2011)  
113 ranging from southern to northern Finland (Fig. 1). Species-level attributes, including the number of stems per hectare, basal  
114 area, mean diameter at breast height, tree height, and length of living crown, were available for the plots. Basal area, the total  
115 cross-sectional area of stemwood (m<sup>2</sup> ha<sup>-1</sup>) at breast height (i.e. at 1.3 m or 1.37 m), is a common measure of stand density in  
116 forest inventories and, combined with information on tree height, used as an indicator of need for silvicultural thinning  
117 operations.

118

119 Tree species in the Alaskan data were coniferous black spruce (*Picea mariana* (Mill.) B. S. P.) and white spruce (*Picea*  
120 *glauca* (Moench) Voss), and broadleaved quaking aspen (*Populus tremuloides* Michx.), black cottonwood or balsam poplar  
121 (*Populus trichocarpa* Torr. & Gray, *P. balsamifera* L.), Alaskan birch (*Betula neolaskana* Sarg.), and Kenai birch (*Betula*  
122 *kenaica* W.H. Evans). Tree species in the Finnish data were coniferous Scots pine (*Pinus sylvestris* L.) and Norway spruce  
123 (*Picea abies* (L.) H. Karst), and broadleaved species comprising mainly of silver and downy birch (*Betula pendula* Roth, *B.*  
124 *pubescens* Ehrh.). The birches accounted for 89% of the basal area of the broadleaved species in Finland. The forest  
125 variables in the study plots are shown in Table 1, for all plots and separately for plots dominated by one species. The  
126 Alaskan and Finnish forests differed in structure. The forests in Alaska were on average denser in terms of basal area (Fig.  
127 2), and contained larger proportion of broadleaved species than the Finnish forests (Table 1). Managed forests in Finland,  
128 which our plots mainly represent, are normally thinned 1–3 times during the rotation period so that coniferous species are  
129 favored. In our plots from Alaska, on the other hand, no thinnings were applied.

130

131 The plots in Finland were classified into six site fertility classes in the field, according to a local site type classification  
132 system (Cajander, 1949). We re-classified the original number of six fertility classes into three: “xeric”, “mesic”, and “herb-  
133 rich”. The cover of grasses is highest in the herb-rich, and decreases towards the xeric type. The cover of lichens, on the

other hand, increases towards the xeric type (Hotanen et al., 2013). In the Alaskan plots no site fertility estimate was available but the cover of each species in the forest floor had been estimated. We labeled the plots as lichen- or grass dominated if either the cover of lichens or the total cover of herbs, grasses, rush, sedges, and fern was over 50%. The remaining plots were dominated by shrubs and mosses or were a mixture of all species groups. Hereafter we refer to these forest floor types as “grass”, “shrub/moss”, and “lichen”. Forest floor types did not differ notably between forests dominated by different tree species, except for Scots pine forests in Finland, which were often found in the xeric type and were almost nonexistent in the herb-rich type (Table 2).

## 2.2 Albedo and FAPAR simulations

### 2.2.1 Simulation model

We simulated albedo and FAPAR using a radiative transfer model called Forest Reflectance and Transmittance model FRT (Kuusk & Nilson, 2000, version modified by Möttus et al., 2007). FRT is a hybrid type model that combines geometric-optical and radiative transfer based sub-models for modeling the first- and higher-order scattering components, respectively. The model has been intercompared and validated within RAdiative transfer Model Intercomparison exercise (RAMI) several times (Widlowski et al., 2007). The advantage of FRT is that it can be parameterized using standard forest inventory data, utilizing the allometric relations of forest variables to foliage biomass and crown dimensions. This was important because field measurements of biophysical variables (e.g., LAI) are not commonly available, as was the case also in our study plots.

FRT simulates stand-level bidirectional reflectance and transmittance factors (BRF, BTF) of a forest at specified wavelengths. A 12×12 Gauss-Legendre cubature was used to integrate the simulated BRF and BTF values over the upper and lower hemispheres, respectively. This resulted in upward scattered and downwelling (directly transmitted or downward scattered) fractions of incoming radiation. The former is observed on top of, and the latter below the tree canopy. These fractions were then used to calculate the shortwave broadband albedo and FAPAR. The simulations were carried out at 5 nm resolution, and the albedo simulations covered a spectral region of 400–2100 nm which corresponds to the region from which input data was available (see Section 2.2.2). The wavelengths below 400 nm account for 8%, and wavelengths over 2100 nm account for 2% of the solar irradiance on top of the atmosphere (Thuillier et al., 2003).

The shortwave albedo was obtained as a weighted sum of the spectral albedos, i.e. upward scattered fractions of incoming radiation ( $f_i$  - ):

$$albedo = \sum_{i=400}^{2100} w_i \times f_i \quad (1)$$

165 The canopy and total FAPAR ( $FAPAR_{CAN}$ ,  $FAPAR_{TOT}$ ) were obtained as weighted sums of canopy absorption ( $a_l^C$ ) and  
 166 total absorption ( $a_l^T$ ) over the PAR region:

167

$$168 \quad FAPAR_{CAN} = \sum_{l=400}^{700} w_l \times a_l^C, \quad (2)$$

169

$$170 \quad FAPAR_{TOT} = \sum_{l=400}^{700} w_l \times a_l^T, \quad (3)$$

171

172

173 The weights ( $w_l$ ) were obtained from the solar irradiance spectrum. Solar irradiance values ( $W\ m^{-2}$ ) were scaled by dividing  
 174 them with the total solar irradiance within the spectral region used (i.e., 400–2100 or 400–700 nm). The weights were thus  
 175 unitless and summed up to unity.  $FAPAR_{TOT}$  and  $FAPAR_{CAN}$  were separated because the former is a measure of total  
 176 ecosystem productivity whereas the latter is more closely linked with timber production. Our  $FAPAR_{CAN}$  and  $FAPAR_{TOT}$  do  
 177 not separate green biomass from woody or dead branches or from litter on the ground, and the values therefore represent  
 178 upper limits of available solar energy for photosynthesis in tree canopy, and in the ecosystem as a whole.

179

180 The canopy and total absorptions needed for FAPAR determination were obtained using upward scattered ( $f_l^-$ ) and  
 181 downwelling ( $f_l^+$ ) fractions of incoming radiation, and the reflectance factor of the forest floor ( $r_g$ ) as follows:

182

$$183 \quad a_l^C = 1 - f_l^+ - f_l^- + r_g \times f_l^+, \quad (4)$$

184

$$185 \quad a_l^T = 1 - f_l^+, \quad (5)$$

186

187 The simulations were carried out assuming direct illumination only (“black-sky”) and completely isotropic diffuse  
 188 illumination (“white-sky”). In both cases, we used a top-of-atmosphere irradiance spectrum (Thuillier et al., 2003) as  
 189 weights. The black-sky albedo and FAPAR were simulated for five SZAs typical for the study areas: 40°, 50°, 60°, 70°, and  
 190 80°. We use terms “small SZA” and “large SZA” to refer to SZAs of 40°–50° and 70°–80°, respectively. Black sky albedo  
 191 is, compared to actual (blue sky) albedo, less dependent on assumptions of atmospheric scattering properties, and is  
 192 commonly used as input in climate modeling (Schaaf et al., 2009). We tested the effect of atmosphere using a simple solar  
 193 spectral model (Bird and Riordan, 1986) for generating at-ground solar irradiance spectrum. Albedo and FAPAR in these  
 194 actual blue-sky conditions were highly correlated ( $r \geq 0.98$ ) with black-sky ones, but blue-sky albedo was higher than

black-sky albedo when SZA was 70° or 80°. This is because scattering in the atmosphere increases as function of SZA. Atmosphere scatters visible more effectively than infrared wavelengths, shifting the irradiance distribution of incoming solar radiation towards longer wavelengths in which vegetation is more reflective. Because of high correlation with black- and blue-sky results, we conclude that inclusion of atmosphere in the calculations would not significantly change the interpretation of our results, although would increase the simulated albedo values at large SZAs.

200

### 201 2.2.2 Model parameters

Tree crowns are represented in the FRT model by geometric primitives (cylinders, cones, ellipsoids, or combinations of them). The foliage within a crown is assumed to be homogeneously distributed. The area volume density (area per unit crown volume) of the foliage depends on the crown dimensions and on the foliage area per tree. Several tree classes can be defined to represent different tree species or size classes. We used one class for each tree species. Because the maximum number of species was seven in the Alaskan data, there was a maximum of seven tree classes per plot. We assumed ellipsoid crown shape. The effect of crown shape on simulated forest BRDF was quantified in Rautiainen et al. (2004) who showed that increasing the crown volume may either increase or decrease the simulated reflectance values, depending on canopy closure. Ellipsoid has been shown to estimate crown volume accurately (Rautiainen et al., 2008) and was therefore used in our study. Crown length was obtained from field measurements, and the crown radius was modeled using species-specific allometric equations that require stem diameter as independent variable (Jakobsons, 1970; Bragg, 2001). Leaf dry biomass was estimated with species-specific biomass equations (Repola, 2008; Repola, 2009; Yarie et al., 2007) and converted into hemisurface i.e. half of total leaf area, using leaf mass per area (LMA) values from literature (Table 3). The performance of wide range of crown radius and foliage mass models in forming the input of FRT has been reported by Lang et al. (2007). The models used in our study were chosen based on geographical proximity to our study areas, and also on model availability, particularly for the Alaskan species for which there existed a limited number of models. A slightly regular spatial distribution pattern of trees was assumed, i.e. a value of 1.2 for the tree distribution parameter (a value of 1 indicates Poisson distribution, Nilson, 1999). Other structural parameters needed in FRT simulations are presented in Table 3.

219

Optical properties i.e. reflectance and transmittance of the leaves and needles were obtained from laboratory spectrometer measurements. The data for Finnish species were from Hyytiälä, Finland (Lukeš et al., 2013b). Spectra of birch were used for all broadleaved species. The data for Alaskan species were from Superior National Forest, Minnesota, USA (Hall et al., 1996). Data for all species could not be found separately, and therefore spectra of black spruce were used for both black and white spruce, spectra of paper birch (*Betula papyrifera* Marsh.) were used for both birch species, and spectra of quaking aspen were used for both quaking aspen and for the black cottonwood/balsam poplar group. Reflectance spectra of black and white spruce needles have been found to be similar at least in the visible and near-infrared wavelengths (Richardson et al., 2003). In our data, the spectra of coniferous species did not differ notably from each other (Fig. 3a). The same applied to



228 broadleaved species. Bark spectra for spruces and *Populus* sp. in Alaska were obtained from Hall et al. (1996), and for Scots  
229 pine and Norway spruce in Finland from Lang et al. (2002) (Fig. 3b). Spectra of birch from Lang et al. (2002) were used for  
230 birches in Alaska and for broadleaved species in Finland.

231

232 We used the annual shoot as a basic scattering element for conifers, similarly as in Lukeš et al. (2013a). This accounts for the  
233 multiple scattering within shoot which results in the shoot albedo being lower than needle albedo. Shoot reflectance and  
234 transmittance spectra were obtained by upscaling the needle single scattering albedo to shoot albedo (Rautiainen et al.,  
235 2012), assuming that the reflectance to transmittance ratio of a shoot is equal to that of a needle. Bi-Lambertian scattering  
236 properties of the scattering elements (leaves or shoots) were assumed.

237

238 Optical properties of the forest floor, i.e. reflectance factors at nadir view were obtained from field spectrometer  
239 measurements. The data were collected from Poker Flat Research Range Black Spruce Forest, Alaska (measurements  
240 described in Yang et al. (2014)), and from Hyytiälä, Finland (using similar methodology as in Rautiainen et al. (2011)).  
241 Separate spectra for each forest floor type was used (Fig. 3c), because characteristics of the forest floor may influence the  
242 forest reflectance and therefore also albedo (Rautiainen et al., 2007).

## 243 **2.3 Data analyses**

### 244 **2.3.1 Albedo, FAPAR, and forest structure**

245 We analyzed albedo and FAPAR ( $FAPAR_{CAN}$ ,  $FAPAR_{TOT}$ ) against each other, and against the forest variables. The analyses  
246 were performed separately for Alaskan and Finnish data, and repeated for all simulated solar illumination conditions.  
247 Because of the strong emphasis on forest management, main focus of the analysis was on tree species and tree height which  
248 are usually measured as part of forest inventories. In addition, we analyzed albedo and FAPAR against effective leaf area  
249 index ( $LAI_{eff}$ ) and above ground biomass (AGB).  $LAI_{eff}$  is calculated by FRT, and corresponds to the LAI of a horizontally  
250 homogeneous, optically turbid canopy that has exactly the same transmittance (gap probability) as the canopy under  
251 examination. AGB was calculated with individual-tree allometric equations (Repola, 2008; Repola, 2009; Yarie et al., 2007),  
252 similarly as the foliage biomass.

253

254 In the next phase, all simulations were repeated assuming black soil (i.e., a totally absorbing background), in order to better  
255 explain the dependencies of albedo on tree height and illumination conditions as well as to explain the differences of albedo  
256 between Alaskan and Finnish forests. The albedo obtained in black soil simulation represents the plain canopy albedo  
257 without the contribution of forest floor vegetation. We refer to this as “canopy contribution”. Correspondingly, the  
258 contribution of forest floor can be calculated by subtracting the canopy contribution from the albedo obtained when  
259 assuming a vegetated forest floor. We refer to this as “forest floor contribution”. Canopy and forest floor contributions can

260 be expressed as absolute values or relative values which sum up to 100%. For comparison with the results regarding albedo,  
261 the forest floor contribution to total ecosystem FAPAR was also calculated, by subtracting  $FAPAR_{CAN}$  from  $FAPAR_{TOT}$ .  
262  
263 We report the relationships of albedo and FAPAR against forest structure in Sect. 3.1. Results of these experiments are  
264 needed for understanding the relations between albedo and FAPAR, which we report in Sect. 3.2.

### 265 2.3.2 Relative importance of density and tree species

266 To examine the relative importance of density and species composition, we analyzed albedo and  $FAPAR_{CAN}$  against basal  
267 area and the proportion of broadleaved trees. The analyses were performed separately for Alaska and Finland, and repeated  
268 for all simulated solar illumination conditions. We excluded all plots with tree height less than 10 m from the analyses in  
269 order to evaluate the effect of basal area independent of tree height. This was done based on the following reasoning. Basal  
270 area was correlated with tree height when studying all plots ( $r = 0.61$  (Alaska),  $r = 0.64$  (Finland)). Preliminary analysis was  
271 performed by successively removing plots with smallest trees and each time checking the correlation between height and  
272 basal area. The correlation was reduced until a height threshold of 10 m ( $r = 0.40$  (Alaska),  $r = 0.34$  (Finland)) (cf. Fig. 2).  
273 Therefore, the 10 m threshold was used to exclude the smallest trees from our analyses. Analysis of albedo and FAPAR  
274 against basal area in this restricted set of plots gives an approximation of how thinnings would affect albedo and  $FAPAR_{CAN}$   
275 although in reality thinning a stand affects not only the basal area but also the spatial pattern and size distribution of trees.

276

277 Mean and standard deviation (SD) of albedo and  $FAPAR_{CAN}$  in conifer-dominated forests were calculated for ten equally  
278 spaced classes with respect to basal area. The center of the lowest class corresponded to the 5th and that of the highest class  
279 to the 95th percentile of basal area in the data. To examine the effect of broadleaved proportion, mean and SD of albedo and  
280  $FAPAR_{CAN}$  were calculated for ten equally spaced classes with respect to proportion of broadleaved trees, i.e. the  
281 broadleaved proportions ranging from 0–10% to 90–100%. The analysis was repeated for sparse (basal area percentiles from  
282 0th to 30th) and dense forest (basal area percentiles from 70th to 100th). We hypothesized that the proportion of broadleaved  
283 trees would have smaller effect on albedo in sparse than in dense forest, because the forest floor has more significant role in  
284 the sparse canopies. Results regarding the analysis of basal area and proportion broadleaved trees are reported in Sect 3.3.

## 285 3 Results

### 286 3.1 Albedo, FAPAR, and forest structure

287 Mean albedo of study plots in Alaska (0.141–0.184) was higher than in Finland (0.136–0.171). In general, the albedo of  
288 broadleaved species was 42–130% higher than that of coniferous (Table 4). However, albedo varied greatly even among  
289 coniferous species: in Alaska, the albedo of black spruce was 19–33% higher than that of white spruce, and in Finland, the  
290 albedo of Scots pine forests was 20–31% higher than that of Norway spruce. Overall, the mean albedo of coniferous species

291 was 28–32% higher in Finland (0.131–0.161) than in Alaska (0.102–0.122). The mean albedos of broadleaved species in  
292 Alaska did not differ significantly from each other ( $p > 0.05$  in ANOVA), except in the white-sky case. Therefore the  
293 broadleaved species were treated as one group hereafter. Increasing the SZA increased the black-sky albedos of all species  
294 (Table 4).

295

296 The forest canopies in Alaska absorbed more PAR radiation than in Finland: mean  $FAPAR_{CAN}$  in Alaska was 0.71–0.92 and  
297 in Finland 0.63–0.89. At the smallest SZA ( $40^\circ$ ) in black-sky simulations,  $FAPAR_{CAN}$  was highest for broadleaved species in  
298 Alaska, followed by Norway spruce in Finland, white spruce in Alaska, and broadleaved in Finland (Table 4). Scots pine in  
299 Finland and black spruce in Alaska had lowest  $FAPAR_{CAN}$  among the species. The mean  $FAPAR_{CAN}$  of broadleaved species  
300 in Alaska did not differ significantly from each other in any of the simulated illumination conditions ( $p > 0.05$  in ANOVA).  
301 Increasing the SZA increased  $FAPAR_{CAN}$  of all species and also reduced the differences between species. The relative  
302 increase was smaller for broadleaved than for coniferous species. Therefore, the order of species in  $FAPAR_{CAN}$  was different  
303 at small and large SZAs (Table 4).  $FAPAR_{TOT}$ , an approximation of total ecosystem productivity, ranged from 0.93 to 0.98  
304 and did not depend strongly on direction of illumination.  $FAPAR_{TOT}$  of coniferous forests was higher than that of  
305 broadleaved but the differences were not large in relative terms because  $FAPAR_{TOT}$  was consistently high.

306

307 White-sky albedo corresponded best with black-sky albedo observed at SZA of  $60^\circ$  ( $r = 0.97$ ,  $RMSE = 0.011$ , mean  
308 difference =  $-0.001$ ). It correlated strongly also with black-sky albedos observed at other SZAs ( $r \geq 0.93$ ). White-sky  
309  $FAPAR_{CAN}$  corresponded best with black-sky  $FAPAR_{CAN}$  observed at SZA of  $40^\circ$  ( $r = 1.00$ ,  $RMSE = 0.04$ , mean difference  
310 =  $0.03$ ) and very closely also with those observed at SZAs of  $50^\circ$  and  $60^\circ$ . On the other hand, it deviated notably from the  
311 black-sky  $FAPAR_{CAN}$  observed at SZAs of  $70^\circ$  and  $80^\circ$ . Because white-sky albedo and FAPAR were highly correlated with  
312 their black-sky counterparts observed at small to moderate SZAs, we report the results hereafter for black-sky conditions  
313 only, except for contribution of forest floor (Table 5) that is presented also for white-sky case, in order to maintain  
314 comparability with results presented in Table 4.

315

316 Albedo decreased with increasing tree height in coniferous forests (Fig. 4). The decrease was most rapid at small tree heights  
317 and saturated after the height reached approximately 10 m. When SZA increased, the difference in albedo between short and  
318 tall forests became smaller (compare Fig. 4a,b to Fig. 4c,d). The albedo of broadleaved forests was similar for all tree heights  
319 at the smallest SZA ( $40^\circ$ ). At large SZAs, however, there was an initial rapid increase in albedo for broadleaved forests with  
320 small trees (Fig. 4d), after which the albedo remained stable. AGB was correlated with tree height ( $r = 0.72$ – $0.78$ ) and the  
321 albedo responded to AGB with a similar saturating trend as in the case of tree height (Fig. 4e,f).

322

323  $FAPAR_{CAN}$  initially increased with increasing tree height, but saturated at large tree heights (Fig. 5). The saturation was  
324 reached earlier and the maximum level of  $FAPAR_{CAN}$  was higher at large SZAs. Similar saturating trends and SZA

dependencies were observed also against AGB although there was less variation in the y direction (Fig. 5e,f).  $FAPAR_{TOT}$  increased as function of tree height in coniferous forests, and was stable in broadleaved forests (Fig. 6). However, the variation in  $FAPAR_{TOT}$  with tree height was small (values ranging from 0.93 to 0.98).

The average contribution of forest floor to total forest albedo depended on tree species and ranged from 4% to 53% (Table 5). It was largest at small SZAs and for tree species that had low  $LAI_{eff}$  (see  $LAI_{eff}$  values in Table 1). Forest floor contribution decreased as a function of tree height (Fig. 7). The relation was even tighter when the forest floor contribution was analyzed against  $LAI_{eff}$  (not shown). This is logical because  $LAI_{eff}$  is more directly linked with canopy transmittance than is tree height. Increasing the SZA increased the canopy contribution in all plots. In general, the net effect was an increase of albedo as a function of SZA. Only a few sparse canopies (low  $LAI_{eff}$ ) were an exception. In these plots, an increase in SZA reduced the forest floor contribution more than it increased the canopy contribution. Results regarding contribution of forest floor to total ecosystem FAPAR were similar as those observed for albedo, i.e. there were differences between tree species and decreasing trends with increasing SZA (Table 5).

The differences in albedos between coniferous species, i.e. black spruce vs. white spruce, and Scots pine vs. Norway spruce, were almost nonexistent when comparing albedos obtained in black soil simulations (Table 5). This indicates that at least some of the differences in albedos between coniferous species are explained by the varying forest floor contribution between species. However, the differences in albedos between coniferous forests of Finland and Alaska remained, indicating that other factors than forest floor influenced the species differences between the study areas.

$FAPAR_{CAN}$  varied notably more than albedo when comparing forests of same height, particularly at small SZAs (Fig. 4, Fig. 5). This can be explained by the link of  $FAPAR_{CAN}$  with canopy interception. Interception was tightly related with  $LAI_{eff}$  (not shown), and it determined  $FAPAR_{CAN}$  almost directly, because the foliage absorbed strongly at PAR wavelengths (Fig. 3a) and therefore the multiple scattering was negligible.  $LAI_{eff}$ , in turn, varied considerably between forests of same height. The outliers (tall trees, low  $FAPAR_{CAN}$ ) in Fig. 5d were plots that had only few trees and therefore very low  $LAI_{eff}$ . Similarly, Scots pine had lower  $FAPAR_{CAN}$  compared to other species with same height (Fig. 5d). Further examination revealed that Scots pine had short crowns and therefore low  $LAI_{eff}$ , although the leaf area per unit crown volume did not differ from the other coniferous species. The strong link between  $FAPAR_{CAN}$  and  $LAI_{eff}$  explained also the observed species- and SZA dependencies of  $FAPAR_{CAN}$ . At the lowest SZA ( $40^\circ$ ) the species-specific  $FAPAR_{CAN}$  (Table 4) was strongly correlated with species-specific  $LAI_{eff}$  (Table 1) ( $r = 0.93$ ). At large SZAs the canopy interception approached 100% at almost all  $LAI_{eff}$  values (cf. Fig. 5c,d) and  $FAPAR_{CAN}$  was therefore mainly determined by the absorption of the foliage at PAR wavelengths. Leaves of broadleaved trees absorbed less than conifer needles, which explains why  $FAPAR_{CAN}$  of broadleaved species did not increase as rapidly as a function of SZA as did  $FAPAR_{CAN}$  of coniferous species (Table 4).

### 358 3.2 Relation of albedo to FAPAR

359 FAPAR<sub>CAN</sub> was negatively correlated with albedo in conifer dominated forests (Fig. 8). The correlation was strongest at the  
360 smallest SZA ( $r = -0.91$ ,  $r = -0.90$ ) and weakest at the largest SZA ( $r = -0.63$ ,  $r = -0.59$ ). When including mixed plots and the  
361 plots dominated by broadleaved trees, correlation of FAPAR<sub>CAN</sub> to albedo varied from almost nonexistent in Alaska ( $r$   
362 ranging from  $-0.17$  to  $0.07$ ) to moderate in Finland ( $r$  ranging from  $-0.62$  to  $-0.30$ ). The higher correlation in Finland can be  
363 explained by the small number of broadleaved dominated forests in our data from Finland. In addition to the proportion of  
364 broadleaved trees, variation in forest floor characteristics influenced the albedo-FAPAR<sub>CAN</sub> relations by altering the albedo  
365 values (Fig. 8). The effect of forest floor was seen in relatively sparse canopies only. For example, at SZA of  $40^\circ$  the effect  
366 of forest floor on albedo started to show at FAPAR<sub>CAN</sub> values below  $0.5$  (Fig. 8). Remembering that FAPAR<sub>CAN</sub> was tightly  
367 related to LAI<sub>eff</sub>, this value corresponds LAI<sub>eff</sub> of approx.  $1$ . FAPAR<sub>TOT</sub> was strongly and negatively correlated with albedo ( $r$   
368 ranging from  $-0.97$  to  $-0.88$ ). The only plots that deviated from this otherwise strong relation were those Scots pine plots that  
369 had low FAPAR<sub>TOT</sub> and xeric forest floor.

### 370 3.3 Relative importance of density and tree species

371 The variation in density of forests was larger in Alaska than in Finland; the 5<sup>th</sup> and 95<sup>th</sup> percentiles of basal area were  $8$  and  
372  $43 \text{ m}^2 \text{ ha}^{-1}$  in Alaska, and  $10$  and  $34 \text{ m}^2 \text{ ha}^{-1}$  in Finland. In both study areas, decrease in basal area resulted in higher albedo  
373 but lower FAPAR<sub>CAN</sub>. At the smallest SZA ( $40^\circ$ ) the decrease in basal area from its 95<sup>th</sup> to 5<sup>th</sup> percentile resulted in increase  
374 of albedo by  $36\%$  in Alaska and by  $21\%$  in Finland (Fig. 9). Correspondingly, FAPAR<sub>CAN</sub> decreased by  $48\%$  in Alaska and  
375 by  $44\%$  in Finland. When SZA increased, the response of FAPAR<sub>CAN</sub> to basal area became weaker. For example, at SZA of  
376  $70^\circ$  the basal area could be reduced to approx.  $20 \text{ m}^2 \text{ ha}^{-1}$  with equal relative changes in albedo and FAPAR<sub>CAN</sub> (Fig. 9b). At  
377 the largest SZA ( $80^\circ$ ) both albedo and FAPAR<sub>CAN</sub> varied very little (max.  $6\%$ ) between the 5<sup>th</sup> and 95<sup>th</sup> basal area  
378 percentiles. In other words, the effect of basal area depended strongly on SZA. However, the relative decrease of FAPAR<sub>CAN</sub>  
379 with decreasing basal area was always larger than or equal to the relative increase in albedo.

380

381 Increasing the proportion of broadleaved trees increased the albedos considerably more than did reduction in basal area (Fig.  
382 9c,d). The effect of broadleaved trees was slightly smaller in sparse than in dense forests. For example, at SZA of  $40^\circ$ ,  
383 increasing the broadleaved proportion from  $0\text{--}10\%$  to  $90\text{--}100\%$  resulted in relative increase of albedo by  $130\%$  (in Alaska)  
384 and  $80\%$  (in Finland) in forests with high basal area (i.e., basal area percentiles from 70th to 100th). In forests with low basal  
385 area (i.e., basal area percentiles from 0th to 30th) the corresponding figures were  $112\%$  (Alaska) and  $71\%$  (Finland). The  
386 smaller relative increase in Finland is explained by the higher albedo of Finnish coniferous forests, because the albedos of  
387 broadleaved species did not differ between Alaska and Finland. FAPAR<sub>CAN</sub> was almost independent on the proportion of  
388 broadleaved trees, except for large SZAs where FAPAR<sub>CAN</sub> tended to decrease slightly when broadleaved proportion

increased (Fig. 9d). This is explained by the fact that at large SZAs  $FAPAR_{CAN}$  was mainly determined by the absorption of canopy elements, and the absorption was lower for broadleaved than for coniferous trees.

#### 4 Discussion

Despite recent studies published on the relationships between albedo and boreal forest structure, and despite the widespread use of FAPAR to monitor vegetation productivity, the physical link between forest albedo and productivity has been poorly understood. To our knowledge, the relationship between these two quantities has not been quantified earlier for an extensive geographical area. Another gap in the discussion has been the role of latitude: solar paths vary across the biome, and therefore, need to be taken into account before making any generalizations on how altering forest structure through silvicultural operations can be used to influence albedo (and furthermore, climate).

Our results show that albedo and  $FAPAR_{CAN}$  are tightly linked in boreal coniferous forests. The prerequisites for this are that there is only a limited proportion of broadleaved trees present in the forest and that the tree canopy is not very sparse (i.e. LAI is not very low). The explanation for the tight connection between albedo and  $FAPAR_{CAN}$  is that they respond with opposite trends to forest structural variables. However, the shapes of these trends depended on directional characteristics of the incoming solar radiation which was also reflected in the albedo vs.  $FAPAR_{CAN}$  relations. This underlines the importance of taking into account latitude and season (i.e. solar angle) when evaluating climate impacts of forests even within one biome.  $FAPAR_{TOT}$  was also tightly linked with albedo. Because  $FAPAR_{TOT}$  equals one minus PAR albedo, this finding indicates that PAR albedo and shortwave albedo of vegetation are correlated. However, the overall variation in  $FAPAR_{TOT}$  was small in magnitude. Our results differ slightly from those observed by Lukeš et al. (2016) who compared satellite-based (MODIS) albedo and FAPAR in Finland and observed much weaker (but still negative) correlation between these quantities. The spatial resolution in their study ( $1 \times 1$  km) was coarser than in our study, and the FAPAR definition differed: MODIS FAPAR is defined as PAR absorbed by green elements of vegetation canopy, both trees and understory included. In addition, Lukeš et al. (2016) did not separate coniferous and broadleaved trees, although this effect is likely minor since the proportion of broadleaved trees is low in Finland. Finally, simulation model used here, although parameterized by field observations, cannot capture all the variability in real forests, and on the other hand, satellite products are likely to include observation and modelling errors that increase the noise in the data.

The responses of albedo to tree species and forest structure were similar across the biome in Alaska and Finland. This corroborates findings in previous, local studies (Amiro et al., 2006; Bright et al., 2013; Lukeš et al., 2014; Kuusinen et al. 2014; Kuusinen et al., 2016). Also the results regarding overall level of  $FAPAR_{CAN}$ , and the dependence of  $FAPAR_{CAN}$  on tree species were similar to earlier studies (Roujean, 1999; Steinberg et al., 2006). However, as our study was based on extensive field data from two continents, drawing more general conclusions on how forest structure, albedo and productivity

421 are interconnected is now possible. In addition, to our knowledge only one study has previously evaluated the forest floor  
422 contribution to albedo (Kuusinen et al., 2015). We showed that forest floor vegetation (which is often in practical forestry  
423 e.g. a proxy for site fertility type) can significantly contribute to forest albedo; its average contribution can be up to 50%,  
424 varying between forests dominated by different tree species. Similarly, the average contribution of forest floor to total  
425 ecosystem FAPAR can be up to or even over 50%, as reported previously also by Ikawa et al. (2015) for an eddy-covariance  
426 study site in Alaska. In other words, even though forest floor vegetation often contributes only little to, for example, total  
427 forest biomass, it can have a significant role as a key driving factor of forest albedo and ecosystem productivity. Quantifying  
428 the variation in forest floor composition and optical properties across the boreal biome constitutes therefore an important  
429 research topic in the future. The important role of forest floor means also that any forest management that influences forest  
430 floor composition can significantly alter the biophysical climate effects of forests. For example, reindeer grazing has been  
431 suggested to reduce land surface albedo, because it reduces the cover of reindeer lichens that have higher albedo compared to  
432 mosses (Stoy et al., 2012).

433

434 The black soil simulations that we conducted in order to quantify the contribution of forest floor explained also why the  
435 albedo increased as a function of solar zenith angle. From previous simulation studies it is known that when the sun  
436 approaches the horizon, the path length of radiation and therefore scattering from the canopy layer increase while the  
437 contribution of forest floor decreases (Kimes et al., 1987; Ni & Woodcock, 2000). The net effect is dependent on the density  
438 (gap fractions) of the canopy layer, and on the reflectance of the forest floor: if the canopy is sparse or clumped, or if the  
439 reflectance of the forest floor is high, it is likely that increasing the solar zenith angle reduces the forest floor contribution  
440 more than it increases the scattering from canopy. Our results generalize the findings of these previous studies that examined  
441 only few stands locally. It should be noted that our results apply only to summertime conditions. If the forest floor has high  
442 reflectance due to e.g. snow cover, a decrease of albedo as a function of solar zenith angle is expected to be observed more  
443 often (Ni & Woodcock, 2000).

444

445 We observed some interesting differences between Alaskan and Finnish datasets which deserve to be highlighted. Even  
446 though our field data do not represent a probability sample they are still well representative of the forests in the study areas.  
447 The mean albedo was higher in Alaska than in Finland, because of the higher proportion of broadleaved species in Alaska.  
448 However, the coniferous forests in Alaska had lower albedos than those in Finland. There is some previous evidence to  
449 support this, because the lowest values reported by Amiro et al. (2006) for spruce forests in Alaska are lower than those  
450 reported by Kuusinen et al. (2014) for spruce in Finland. Because the difference remained also when assuming black soil, the  
451 reason is in the properties of the canopy layer. Particularly, the low reflectance of bark in the Alaskan species (Fig. 3b)  
452 explains part of the difference.

453

454 Radiative transfer models offer a useful tool for assessing the radiation regime of forests, especially when the modeling  
455 approach can utilize readily available common forest inventory databases. Validating the simulated albedo and FAPAR  
456 values, however, is challenging. Even though international model intercomparison efforts such as RAMI (Widlowski et al.,  
457 2007) provide a rigorous set of reports on performance of radiative transfer models, the quality of available input data in  
458 each study where a radiative transfer model is applied is crucial. For example, the forest floor albedos that we calculated  
459 from the available reflectance spectra (Fig. 3) were clearly higher (0.18–0.23) than forest floor albedos measured in the field  
460 at other boreal sites (approx. 0.15 in Manninen & Riihelä, 2008; Manninen & Riihelä, 2009; Kuusinen et al., 2014). If we  
461 had scaled our reflectance factors in order to obtain forest floor albedos of 0.15, the simulated forest albedos would have  
462 decreased by 7–10%. Furthermore, including also the UV region in the simulations would have reduced the simulated  
463 albedos by up to 7%, assuming that the optical properties of the canopy and forest floor are similar at UV than at 400 nm.  
464 However, particularly the lack of field measured spectra for some of the Alaskan species is a limitation of our study and  
465 shows that there is an urgent need for comprehensive spectral database of boreal tree species.

466

467 Our results regarding basal area give an idea of the magnitude of the effects that varying thinning regimes could have on  
468 forest albedo and productivity. The effect of thinnings on albedo have previously been estimated mainly by in situ  
469 measurements at few selected sites (Kirschbaum et al., 2011; Kuusinen et al., 2014). In our study, reduction in the basal area  
470 reduced FAPAR<sub>CAN</sub> equally or more compared to how albedo changed. In contrast to basal area, the proportion of  
471 broadleaved trees had a notably larger effect on forest albedo while having only a negligible influence on forest productivity  
472 (FAPAR<sub>CAN</sub>). The relative importance of basal area and tree species nevertheless depends on the spectral properties of the  
473 tree species and forest floor. Based on our results, the effect of thinning (removal of basal area) on albedo and FAPAR  
474 depends on solar angle. Therefore, the influence of thinning on forest productivity differs between latitudes. Furthermore,  
475 because the basal area influenced albedo and FAPAR<sub>CAN</sub> less at large sun zenith angles, the effects of thinning integrated  
476 over entire rotation period may not be as large as they seem when studying them only at solar noon.

477

478 Global satellite products have provided us insight on coarse-scale trends of albedo in different biomes. However, their  
479 weakness is that even though we can establish correlations between changes in albedo and changes in land cover, we are still  
480 not able to identify and quantify the biophysical factors which cause the albedo of a forest area to change. In addition, a  
481 specific challenge in coupling forest management operations with changes in satellite-based albedo products is that the scale  
482 of these operations significantly differs in North America and Northern Europe, and often does not directly correspond to the  
483 spatial resolution of current albedo products. With an understanding of the consequences of, for example, forest management  
484 practices on the albedo, best-practice recommendations for forest management in future climate mitigation policies will  
485 become more justified. By coupling extensive field inventory data sets and radiative transfer modeling, we showed that  
486 albedo and FAPAR<sub>CAN</sub> are tightly linked in boreal coniferous forests at stand level. However, the relation is weaker if the  
487 forest has deciduous admixture, or if the canopies are sparse and at the same time the species composition (i.e. optical



properties) of the forest floor vary. Because the shape of the relationship between albedo and  $FAPAR_{CAN}$  was shown to depend on solar angle, studies evaluating the climate effects of forest management strategies need to consider latitudinal effects due to varying solar paths. The comparisons between Alaska and Finland revealed that albedo and  $FAPAR_{CAN}$  differ between geographical regions because of the differences in forest structure. However, regardless of geographical region in the boreal zone, the potential of using thinning to increase forest albedo may be limited compared to the effect of favoring broadleaved species.

#### **Data availability**

Data from Co-operative Alaska Forest Inventory prior to 2009 are available at LTER Network Data Portal (<http://dx.doi.org/10.6073/pasta/d442e829a1adf7da169b6076826de563>). Forest inventory data from Finland are described in Korhonen (2011) and Majasalmi et al. (2015). Leaf and needle optical properties measured in Hyytiälä are repositied at SPECCHIO database (<http://www.specchio.ch/>), and those measured in Superior National Forest are repositied at ORNL DAAC by NASA (<http://dx.doi.org/10.3334/ORNLDAAC/183>). Forest floor spectra were presented in Fig. 3 of this manuscript.

#### **Acknowledgments**

This study was funded in parts by the Academy of Finland projects BOREALITY and SATLASER, and by the Davis College of Agriculture, Natural Resources & Design, West Virginia University, under the US Department of Agriculture (USDA) McIntire–Stennis Funds WVA00106. We thank Petr Lukeš and Matti Möttöus for advice on radiative transfer modeling, and Titta Majasalmi, Pekka Voipio, Jussi Peuhkurinen and Maria Villikka for organizing the measurements of field plots in Finland. We also thank the School of Natural Resources and Agricultural Sciences, University of Alaska for the establishment and maintenance of the Co-operative Alaska Forest Inventory. The forest floor reflectances at Poker Flag Research Range were obtained under the JAMSTEC and IARC/UAF collaborative study (PI: Rikie Suzuki).

#### **References**

- Alkama, R. and Cescatti, A.: Biophysical climate impacts of recent changes in global forest cover, *Science*, 351, 600–604, 2016.
- Amiro, B. D., Orchansky, A. L., Barr, A. G., Black, T. A., Chambers, S. D., Chapin, F. S., Goulden, M. L., Litvak, M., Liu, H. P., McCaughey, J. H., McMillan, A. and Randerson, J. T.: The effect of post-fire stand age on the boreal forest energy balance, *Agric. For. Meteorol.*, 140, 41–50, 2006.

515 Bird, R. E. and Riordan, C.: Simple Solar Spectral Model for Direct and Diffuse Irradiance on Horizontal and Tilted Planes  
516 at the Earth's Surface for Cloudless Atmospheres, *J. Clim. Appl. Meteorol.*, 25, 87–97, 1986. Bond-Lamberty, B., Wang, C.,  
517 Gower, S. T. and Norman, J.: Leaf area dynamics of a boreal black spruce fire chronosequence., *Tree Physiol.*, 22, 993–  
518 1001, 2002.

519 Bragg, D. C.: A local basal area adjustment for crown width prediction, *North. J. Appl. For.*, 18, 22–28, 2001.

520 Bright, R. M., Antón-Fernández, C., Astrup, R., Cherubini, F., Kvalevåg, M. and Strømman, A. H.: Climate change  
521 implications of shifting forest management strategy in a boreal forest ecosystem of Norway, *Glob. Chang. Biol.*, 20, 607–  
522 621, 2014.

523 Bright, R. M., Astrup, R. and Strømman, A. H.: Empirical models of monthly and annual albedo in managed boreal forests  
524 of interior Norway, *Clim. Change*, 120, 183–196, 2013.

525 Cajander, A. K.: Forest types and their significance. *Acta Forestalia Fennica*, 56, 1–71, 1949.

526 Chasmer, L., Hopkinson, C., Treitz, P., McCaughey, H., Barr, A. and Black, A.: A lidar-based hierarchical approach for  
527 assessing MODIS fPAR, *Remote Sens. Environ.*, 112, 4344–4357, 2008.

528 Gobron, N., Verstraete, M.M.: Assessment of the status of the development of the standards for the terrestrial essential  
529 climate variables. T10 Fraction of Absorbed Photosynthetically Active Radiation (FAPAR). V8, GTOS65, pp. 1–24. NRC,  
530 FAO, Rome, Italy, 2009.

531 Hall, F. G., Huemmrich, K. F., Strebel, D. E., Goetz, S. J., Nickeson, J. E., and Woods, K. D.: SNF Leaf Optical Properties:  
532 Cary-14. [Superior National Forest Leaf Optical Properties: Cary-14]. Data set. Available on-line [<http://www.daac.ornl.gov>]  
533 from Oak Ridge National Laboratory Distributed Active Archive Center, Oak Ridge, Tennessee, U.S.A, 1996. Based on  
534 Hall, F. G., Huemmrich, K. F., Strebel, D. E., Goetz, S. J., Nickeson, J. E., and Woods, K. D.: Biophysical, Morphological,  
535 Canopy Optical Property, and Productivity Data from the Superior National Forest, NASA Technical Memorandum 104568,  
536 National Aeronautics and Space Administration, Goddard Space Flight Center, Greenbelt, Maryland, U.S.A., 1992.  
537 doi:10.3334/ORNLDAAAC/183

538 Hotanen, J-P., Nousiainen, H., Mäkipää, R., Reinikainen, A., Tonteri, T.: Metsätyypit – opas kasvupaikkojen luokitteluun (In  
539 Finnish), pp. 1–192. Metsäkustannus Oy, Porvoo, Finland, 2013.

540 Ikawa, H., Nakai, T., Busey, R. C., Kim, Y., Kobayashi, H., Nagai, S., Ueyama, M., Saito, K., Nagano, H., Suzuki, R. and  
541 Hinzman, L.: Understory CO<sub>2</sub>, sensible heat, and latent heat fluxes in a black spruce forest in interior Alaska, *Agric. For.*  
542 *Meteorol.*, 214–215, 80–90, 2015.

543 Jakobsons, A.: Sambandet mellan trädkronans diameter och andra trädfaktorer, främst brösthöjdsdiametern: analyser  
544 grundade på riksskogstaxeringens provträdsmaterial (the relationship between crown diameter and other tree factors,

diameter at breast height in particular: analysis based on the sample tree material of the National Forest Inventory).

Stockholms skoghögsskolan, institutionen för skogstaxering (Rapporter och uppsatser 14), pp.1–75, 1970.

Kimes, D. S., Sellers, P. J. and Newcomb, W. W.: Hemispherical reflectance variations of vegetation canopies and implications for global and regional energy budget studies, *J. Clim. Appl. Meteorol.*, 26, 959–972, 1987.

Kirschbaum, M. U. F., Whitehead, D., Dean, S. M., Beets, P. N., Shepherd, J. D. and Ausseil, A. G. E.: Implications of albedo changes following afforestation on the benefits of forests as carbon sinks, *Biogeosciences*, 8, 3687–3696, 2011.

Korhonen, L.: Estimation of boreal forest canopy cover with ground measurements, statistical models and remote sensing. *Dissertationes Forestales*, 115, 1–56, 2011.

Kull, O. and Niinemets, U.: Variations in Leaf Morphometry and Nitrogen Concentration in *Betula-Pendula* Roth, *Corylus-Avellana* L and *Lonicera-Xylosteum* L, *Tree Physiol.*, 12, 311–318, 1993.

Kuusinen, N., Kolari, P., Levula, J., Porcar-Castell, A., Stenberg, P. and Berninger, F.: Seasonal variation in boreal pine forest albedo and effects of canopy snow on forest reflectance, *Agric. For. Meteorol.*, 164, 53–60, 2012.

Kuusinen, N., Tomppo, E. and Berninger, F.: Linear unmixing of MODIS albedo composites to infer subpixel land cover type albedos, *Int. J. Appl. Earth Obs. Geoinf.*, 23, 324–333, 2013.

Kuusinen, N., Lukeš, P., Stenberg, P., Levula, J., Nikinmaa, E. and Berninger, F.: Measured and modelled albedos in Finnish boreal forest stands of different species, structure and understory, *Ecol. Modell.*, 284, 10–18, 2014.

Kuusinen, N., Stenberg, P., Tomppo, E., Bernier, P., Berninger, F., Kuusinen, N., Stenberg, P., Berninger, F., Tomppo, E. and Bernier, P.: Variation in understory and canopy reflectance during stand development in Finnish coniferous forests, *Can. J. For. Res.*, 45, 1077–1085, 2015.

Kuusinen, N., Stenberg, P., Korhonen, L., Rautiainen, M. and Tomppo, E.: Structural factors driving boreal forest albedo in Finland, *Remote Sens. Environ.*, 175, 43–51, 2016.

Kuusk, A. and Nilson, T.: A directional multispectral forest reflectance model, *Remote Sens. Environ.*, 72, 244–252, 2000.

Lang, M., Kuusk, A., Nilson, T., Lökk, T., Pehk, M., Alm, G.: Reflectance spectra of ground vegetation in sub-boreal forests. Web page. Available online. <http://www.aai.ee/bgf/ger2600/> (from Tartu Observatory, Estonia. Accessed 6 Feb, 2013), 2002.

Lang, M., Nilson, T., Kuusk, A., Kiviste, A. and Hordo, M.: The performance of foliage mass and crown radius models in forming the input of a forest reflectance model: A test on forest growth sample plots and Landsat 7 ETM+ images, *Remote Sens. Environ.*, 110, 445–457, 2007.

573 Liang, J., Zhou, M., Tobin, P. C., McGuire, A. D. and Reich, P. B.: Biodiversity influences plant productivity through niche-  
574 efficiency., *Proc. Natl. Acad. Sci. U. S. A.*, 112, 5738–5743, 2015.

575 Lukeš, P., Stenberg, P. and Rautiainen, M.: Relationship between forest density and albedo in the boreal zone, *Ecol. Modell.*,  
576 261–262, 74–79, 2013a.

577 Lukeš, P., Stenberg, P., Rautiainen, M., Möttus, M. and Vanhatalo, K. M.: Optical properties of leaves and needles for boreal  
578 tree species in Europe, *Remote Sens. Lett.*, 4, 667–676, 2013b.

579 Lukeš, P., Rautiainen, M., Manninen, T., Stenberg, P. and Möttus, M.: Geographical gradients in boreal forest albedo and  
580 structure in Finland, *Remote Sens. Environ.*, 152, 526–535, 2014.

581 Lukeš, P., Stenberg, P., Möttus, M. and Manninen, T.: Multidecadal analysis of forest growth and albedo in boreal Finland,  
582 *Int. J. Appl. Earth Obs. Geoinf.*, 52, 296–305, 2016.

583 Majasalmi, T., Rautiainen, M. and Stenberg, P.: Modeled and measured fPAR in a boreal forest: Validation and application  
584 of a new model, *Agric. For. Meteorol.*, 189–190, 118–124, 2014.

585 Majasalmi, T., Rautiainen, M., Stenberg, P. and Manninen, T.: Validation of MODIS and GEOV1 fPAR Products in a  
586 Boreal Forest Site in Finland, *Remote Sens.*, 7, 1359–1379, 2015.

587 Malone, T., Liang, J., Packee, E.C.: Cooperative Alaska Forest Inventory. General Technical Report PNW-GTR-785, USDA  
588 Forest Service, Pacific Northwest Research Station, 32 Portland, OR, pp. 1–58, 2009.

589 Manninen, T., Riihelä, A.: Subarctic boreal forest albedo estimation using ENVISAT ASAR for BRDF determination.  
590 *Proceedings of IGARSS’08*, July 6 11, 2008, CD, p. 1–4, 2008.

591 Manninen, T., Riihelä, A.: ENVISAT/ASAR VV/HH backscattering and the radiation characteristics of Subarctic boreal  
592 forest. *Proceedings of PolInSAR 2009*, 26–30 January 2009, Frascati, Italy, Special publication of ESA SP-668, pp. 1–8,  
593 2009.

594 Monteith, J. L.: Solar radiation and productivity in tropical ecosystems. *Journal of Applied Ecology*, 9, 744–766, 1972.

595 Möttus, M., Stenberg, P. and Rautiainen, M.: Photon recollision probability in heterogeneous forest canopies: Compatibility  
596 with a hybrid GO model, *J. Geophys. Res. Atmos.*, 112, 1–10, 2007.

597 Naudts, K., Chen, Y., McGrath, M. J., Ryder, J., Valade, A., Otto, J., Luyssaert, S.: Europe’s forest management did not  
598 mitigate climate warming. *Science*, 351, 597–601, 2016.

599 Ni, W. and Woodcock, C. E.: Effect of canopy structure and the presence of snow on the albedo of boreal conifer forests, *J.*  
600 *Geophys. Res.*, 105, 11879, 2000.

601 Nilson, T.: Inversion of gap frequency data in forest stands, *Agric. For. Meteorol.*, 98–9, 437–448, 1999.

602 Palmroth, S. and Hari, P.: Evaluation of the importance of acclimation of needle structure, photosynthesis, and respiration to  
603 available photosynthetically active radiation in a Scots pine canopy, *Can. J. For. Res.*, 31, 1235–1243, 2001.

604 Pan, Y., Birdsey, R. A., Fang, J., Houghton, R., Kauppi, P. E., Kurz, W. A., Phillips, O. L., Shvidenko, A., Lewis, S. L.,  
605 Canadell, J. G., Ciais, P., Jackson, R. B., Pacala, S. W., McGuire, A. D., Piao, S., Rautiainen, A., Sitch, S. and Hayes, D.: A  
606 Large and Persistent Carbon Sink in the World's Forests, *Science*, 333, 988–993, 2011.

607 Rautiainen, M., Suomalainen, J., Möttus, M., Stenberg, P., Voipio, P., Peltoniemi, J. and Manninen, T.: Coupling forest  
608 canopy and understory reflectance in the Arctic latitudes of Finland, *Remote Sens. Environ.*, 110, 332–343, 2007.

609 Rautiainen, M., Mottus, M., Stenberg, P. and Ervasti, S.: Crown envelope shape measurements and models, *Silva Fenn.*, 42,  
610 19–33, 2008.

611 Rautiainen, M., Möttus, M., Heiskanen, J., Akujärvi, A., Majasalmi, T. and Stenberg, P.: Seasonal reflectance dynamics of  
612 common understory types in a northern European boreal forest, *Remote Sens. Environ.*, 115, 3020–3028, 2011.

613 Rautiainen, M., Möttus, M., Yáñez-Rausell, L., Homolová, L., Malenovský, Z. and Schaepman, M. E.: A note on upscaling  
614 coniferous needle spectra to shoot spectral albedo, *Remote Sens. Environ.*, 117, 469–474, 2012.

615 Rautiainen, M., Stenberg, P., Nilson, T. and Kuusk, A.: The effect of crown shape on the reflectance of coniferous stands,  
616 *Remote Sens. Environ.*, 89, 41–52, 2004.

617 Reich, P. B., Ellsworth, D. S., Walters, M. B., Vose, J. M., Gresham, C., Volin, J. C. and Bowman, W. D.: Generality of leaf  
618 trait relationships: A test across six biomes, *Ecology*, 80, 1955–1969, 1999.

619 Repola, J.: Biomass equations for birch in Finland, *Silva Fenn.*, 42, 605–624, 2008.

620 Repola, J.: Biomass equations for Scots pine and Norway spruce in Finland, *Silva Fenn.*, 43, 625–647, 2009.

621 Richardson, A. D., Berlyn, G. P. and Duigan, S. P.: Reflectance of Alaskan black spruce and white spruce foliage in relation  
622 to elevation and latitude, *Tree Physiol.*, 23, 537–544, 2003.

623 Roujean, J. L.: Measurements of PAR transmittance within boreal forest stands during BOREAS, *Agric. For. Meteorol.*, 93,  
624 1–6, 1999.

625 Schaaf, C. B.: Assessment of the status of the development of the standards for the terrestrial essential climate variables. T8  
626 albedo and reflectance anisotropy. V12, GTOS63, pp. 1–20 NRC, FAO, Rome, 2009.

627 Serbin, S. P., Ahl, D. E. and Gower, S. T.: Spatial and temporal validation of the MODIS LAI and FPAR products across a  
628 boreal forest wildfire chronosequence, *Remote Sens. Environ.*, 133, 71–84, 2013.

629 Sigurdsson, B. D., Thorgeirsson, H. and Linder, S.: Growth and dry-matter partitioning of young *Populus trichocarpa* in  
630 response to carbon dioxide concentration and mineral nutrient availability., *Tree Physiol.*, 21, 941–50, 2001.

631 Smolander, H., Stenberg, P. and Linder, S.: Dependence of light interception efficiency on structural parameters, *Tree*  
632 *Physiol.*, 14, 971–980, 1994.

633 Steinberg, D., Goetz, S. and Hyer, E.: Validation of MODIS FPAR products in boreal forests of Alaska, *IEEE Trans. Geosci.*  
634 *Remote Sens.*, 44, 1818–1828, 2006.

635 Stenberg, P., Kangas, T., Smolander, H. and Linder, S.: Shoot structure, canopy openness, and light interception in Norway  
636 spruce, *Plant, Cell Environ.*, 22, 1133–1142, 1999.

637 Stenberg, P., Linder, S. and Smolander, H.: Variation in the ratio of shoot silhouette area to needle area in fertilized and  
638 unfertilized Norway spruce trees., *Tree Physiol.*, 15, 705–12, 1995.

639 Stoy, P. C., Street, L. E., Johnson, A. V, Prieto-Blanco, A. and Ewing, S. A.: Temperature, heat flux, and reflectance of  
640 common subarctic mosses and lichens under field conditions: might changes to community composition impact climate-  
641 relevant surface fluxes?, *Arct. Antarct. Alp. Res.*, 44, 500–508, 2012.

642 Th  r  zien, M., Palmroth, S., Brady, R. and Oren, R.: Estimation of light interception properties of conifer shoots by an  
643 improved photographic method and a 3D model of shoot structure., *Tree Physiol.*, 27, 1375–87, 2007.

644 Thuillier, G., Hers, M., Simon, P. C., Labs, D., Mandel, H. and Gillotay, D.: Observation of the solar spectral irradiance  
645 from 200 nm to 870 nm during the ATLAS 1 and ATLAS 2 missions by the SOLSPEC spectrometer, *Metrologia*, 35, 689–  
646 695, 2003.

647 Widlowski, J. L., Taberner, M., Pinty, B., Bruniquel-Pinel, V., Disney, M., Fernandes, R., Gastellu-Etchegorry, J. P.,  
648 Gobron, N., Kuusk, A., Lavergne, T., Leblanc, S., Lewis, P. E., Martin, E., M  ttus, M., North, P. R. J., Qin, W., Robustelli,  
649 M., Rochdi, N., Ruiloba, R., Soler, C., Thompson, R., Verhoef, W., Verstraete, M. M. and Xie, D.: Third Radiation Transfer  
650 Model Intercomparison (RAMI) exercise: Documenting progress in canopy reflectance models, *J. Geophys. Res. Atmos.*,  
651 112, 1–28, 2007.

652 Yang, W., Kobayashi, H., Suzuki, R. and Nasahara, K.: A Simple Method for Retrieving Understory NDVI in Sparse  
653 Needleleaf Forests in Alaska Using MODIS BRDF Data, *Remote Sens.*, 6, 11936–11955, 2014.

654 Yarie, B. J., Kane, E., Hall, B.: Aboveground Biomass Equations for the Trees of Interior Alaska. *AFES Bulletin*, 115, 1–16,  
655 2007.

656 Table 1. Mean (standard deviation) of forest variables by dominant tree species in Alaska and Finland. The species  
657 dominance was determined by basal area proportion: If the basal area of one of the species exceeded 80% of the total basal  
658 area, the plot was considered to be dominated by that species. The remaining plots were labeled as mixed.

Tree species	Number of plots	Stems per hectare	Diameter at breast height (cm) <sup>1)</sup>	Height (m)	Crown ratio (%) <sub>2)</sub>	Basal area (m <sup>2</sup> ha <sup>-1</sup> )	Effective LAI (m <sup>2</sup> m <sup>-2</sup> ) <sub>3)</sub>
Alaska							
Black spruce	70	2361 (1542)	9.3 (3.8)	7.3 (3.2)	69 (11)	14.6 (9.3)	1.0 (0.6)
White spruce	124	806 (653)	21.3 (7.9)	14.7 (5.2)	74 (9)	22.8 (13.1)	2.4 (1.3)
Quaking aspen	22	1572 (916)	15.8 (5.1)	13.9 (3.5)	37 (7)	26.0 (8.8)	2.8 (0.9)
Black cottonwood/ balsam poplar	8	672 (658)	35.1 (14.7)	20.5 (5.8)	62 (11)	34.8 (14.5)	2.7 (1.1)
Birches	84	873 (662)	22.6 (8.4)	17.5 (2.9)	58 (11)	25.1 (8.1)	3.2 (1.4)
Mixed	276	1082 (1131)	22.0 (8.3)	15.1 (3.9)	62 (12)	25.2 (10.1)	2.7 (1.2)
All	584	1160 (1139)	20.3 (9.0)	14.4 (4.9)	64 (13)	23.6 (11.0)	2.5 (1.3)
Finland							
Scots pine	184	1165 (1301)	18.0 (8.5)	14.7 (6.4)	51 (16)	15.9 (7.7)	1.1 (0.5)
Norway spruce	115	980 (1014)	19.7 (8.9)	16.6 (6.9)	68 (15)	19.8 (9.4)	2.4 (1.1)
Broadleaved	23	1409 (1419)	13.6 (7.1)	13.9 (6.0)	62 (16)	12.6 (7.1)	1.9 (1.2)
Mixed	180	1094 (1782)	20.5 (8.0)	17.2 (5.8)	58 (14)	20.3 (9.1)	2.2 (1.1)
All	502	1109 (1444)	19.1 (8.5)	16.0 (6.4)	58 (16)	18.2 (8.9)	1.8 (1.1)

659 1) Definition of breast height differed between Alaska (1.37 m) and Finland (1.3 m).

660 2) Ratio of the length of living crown to tree height.

661 3) Not measured in the field. The values are calculated by the FRT model.

662 Table 2. Number of study plots by dominant tree species and forest floor type. The species dominance was determined by  
663 basal area proportion: If the basal area of one of the species exceeded 80% of the total basal area, the plot was considered to  
664 be dominated by that species.

Tree species	Forest floor		
	Grass	Shrub/moss	Lichen
Black spruce	8	60	2
White spruce	13	111	0
Quaking aspen	4	18	0
Black cottonwood/balsam poplar	2	6	0
Birches	23	61	0
Mixed	40	236	0
All	90	492	2
	Herb-rich	Mesic	Xeric
Scots pine	2	145	37
Norway spruce	28	86	1
Broadleaved	8	14	1
Mixed	26	152	2
All	64	397	41

665





674 Table 4. Albedo,  $FAPAR_{CAN}$ , and  $FAPAR_{TOT}$  by dominant tree species and SZA. The reported value for given species is the  
675 mean of plots in which the basal area proportion of that species exceeded 80%. The number of plots and mean forest  
676 variables for each species are reported in Table 1.

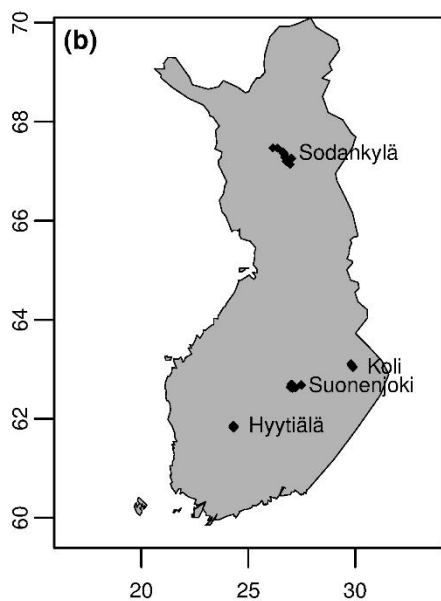
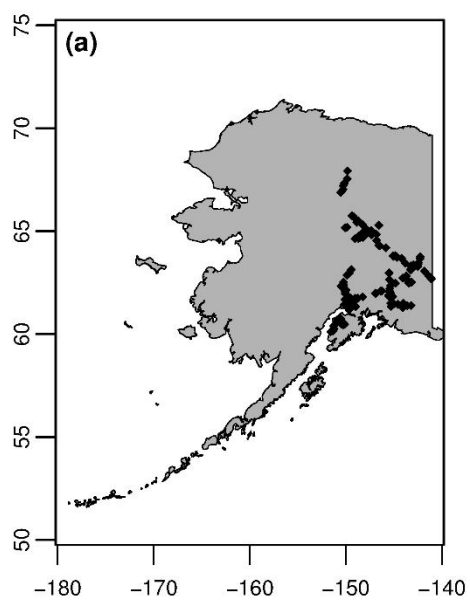
Tree species	Black-sky (SZA)					White-sky
	40°	50°	60°	70°	80°	
Albedo						
Black spruce	0.121	0.122	0.124	0.128	0.137	0.124
White spruce	0.091	0.094	0.097	0.103	0.114	0.104
Broadleaved (Alaska)	0.194	0.204	0.218	0.236	0.262	0.205
Scots pine	0.144	0.147	0.152	0.159	0.172	0.151
Norway spruce	0.110	0.114	0.120	0.128	0.141	0.126
Broadleaved (Finland)	0.207	0.218	0.231	0.248	0.273	0.224
FAPAR <sub>CAN</sub>						
Black spruce	0.47	0.53	0.61	0.72	0.86	0.53
White spruce	0.72	0.77	0.84	0.90	0.95	0.74
Broadleaved (Alaska)	0.78	0.82	0.86	0.89	0.91	0.80
Scots pine	0.50	0.57	0.65	0.75	0.86	0.55
Norway spruce	0.73	0.79	0.84	0.89	0.92	0.74
Broadleaved (Finland)	0.60	0.65	0.71	0.76	0.81	0.62
FAPAR <sub>TOT</sub>						
Black spruce	0.97	0.97	0.97	0.97	0.97	0.97
White spruce	0.98	0.98	0.98	0.98	0.98	0.98
Broadleaved (Alaska)	0.95	0.95	0.94	0.94	0.93	0.95
Scots pine	0.97	0.97	0.97	0.97	0.96	0.96
Norway spruce	0.97	0.97	0.97	0.97	0.97	0.97
Broadleaved (Finland)	0.95	0.95	0.94	0.94	0.93	0.94

677

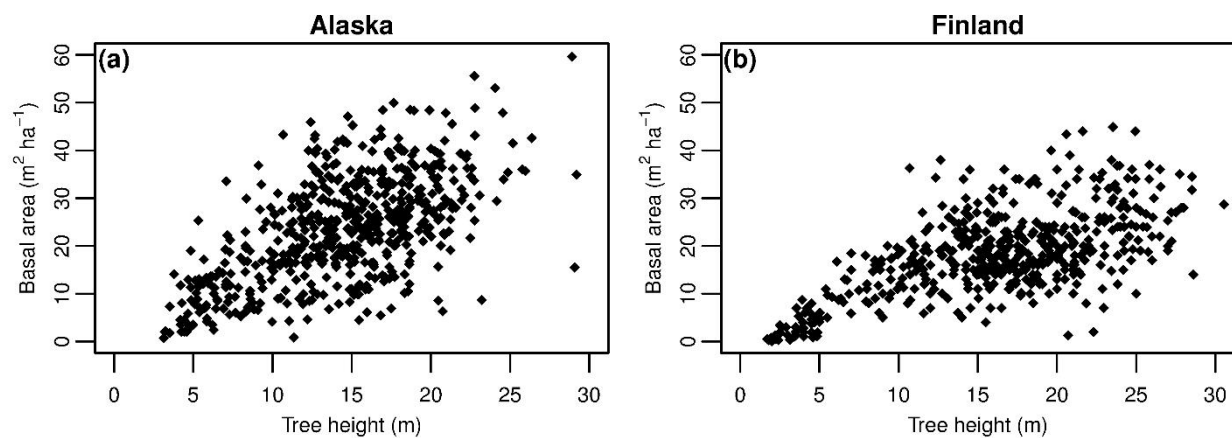
678 Table 5. Canopy and forest floor contributions to albedo, and forest floor contribution to FAPAR<sub>TOT</sub> by dominant tree  
679 species and SZA. The reported value for given species is the mean of plots in which the basal area proportion of that species  
680 exceeded 80%. Note that the values are directly comparable to the species specific forest albedos and FAPAR values  
681 reported in Table 4, i.e. exactly the same plots were used to calculate the average values in both tables.

Tree species	Black-sky (SZA)					White-sky
	40°	50°	60°	70°	80°	
Forest albedo when assuming black soil						
Black spruce	0.053	0.059	0.069	0.084	0.108	0.066
White spruce	0.062	0.068	0.076	0.087	0.104	0.081
Broadleaved (Alaska)	0.169	0.182	0.199	0.221	0.251	0.186
Scots pine	0.075	0.084	0.096	0.114	0.140	0.094
Norway spruce	0.079	0.087	0.097	0.109	0.128	0.102
Broadleaved (Finland)	0.140	0.155	0.173	0.197	0.231	0.165
Contribution of forest floor to total forest albedo, %						
Black spruce	52.9	48.0	41.4	32.4	20.2	46.8
White spruce	27.9	23.7	19.0	13.7	8.0	22.1
Broadleaved (Alaska)	12.9	10.9	8.7	6.5	4.3	9.3
Scots pine	45.6	40.6	34.5	26.8	17.9	37.7
Norway spruce	23.5	19.7	15.8	11.9	8.0	19.0
Broadleaved (Finland)	32.7	29.5	25.9	21.9	17.1	26.3
Contribution of forest floor to FAPAR <sub>TOT</sub> , %						
Black spruce	50.1	44.1	36.0	25.1	11.1	45.7
White spruce	26.4	20.6	14.5	8.3	2.6	24.3
Broadleaved (Alaska)	16.9	12.5	8.3	4.6	2.0	15.9
Scots pine	46.3	39.8	31.7	21.5	10.5	42.8
Norway spruce	24.4	18.7	13.2	8.3	4.4	23.3
Broadleaved (Finland)	34.7	29.3	23.5	17.7	12.4	34.3

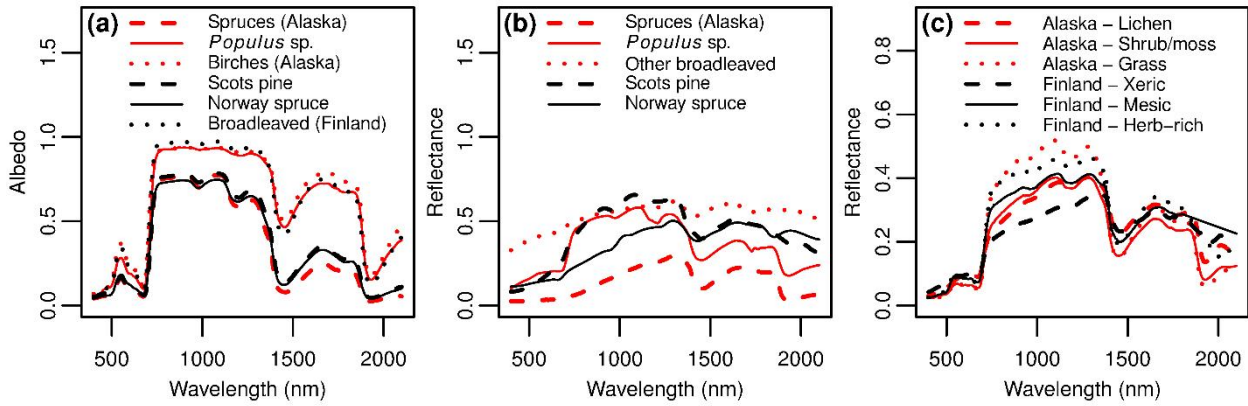
682



683  
684 Figure 1. Location of the field plots.

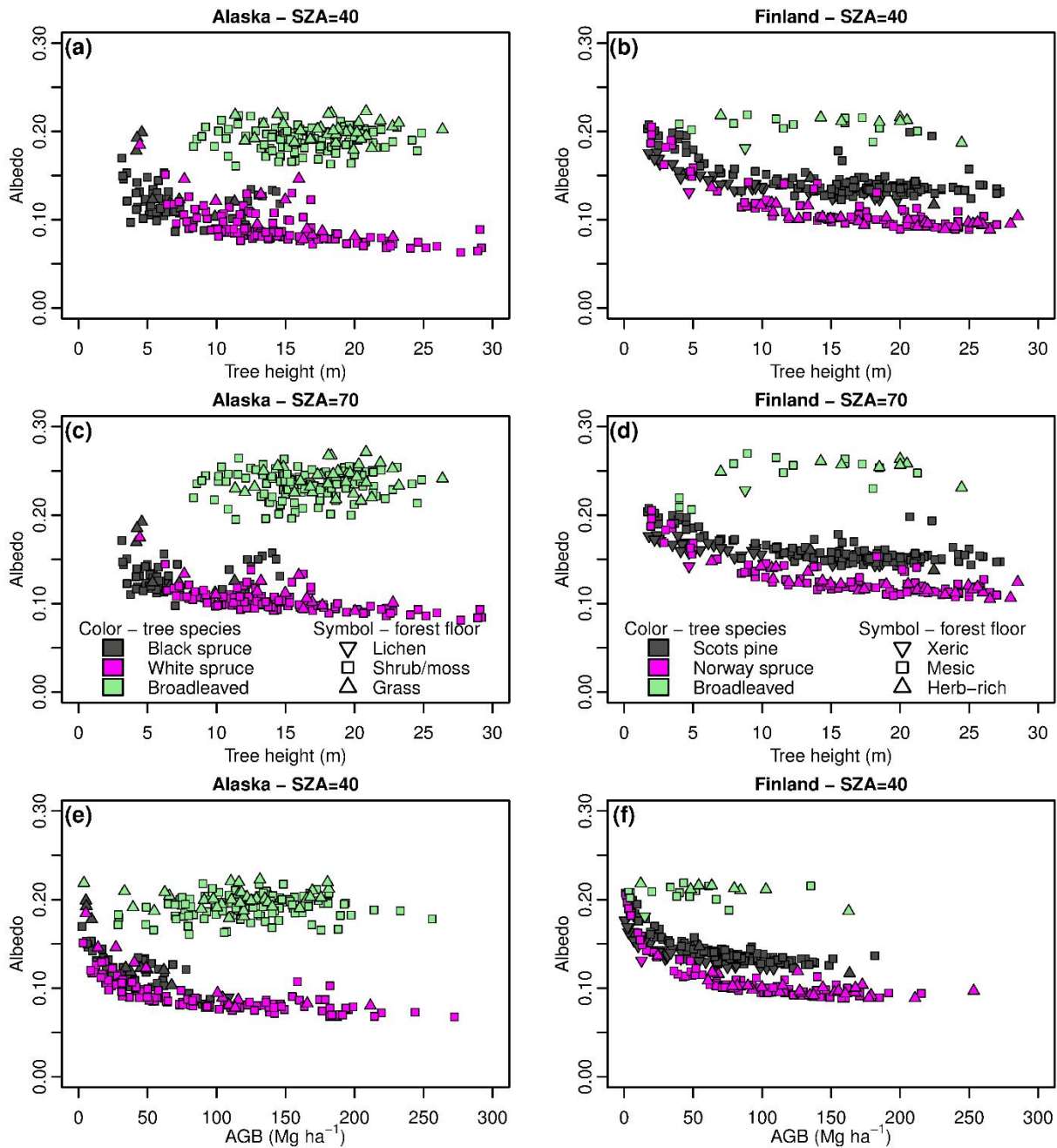


685  
686 Figure 2. Basal area against tree height in the study plots in Alaska (a) and Finland (b).



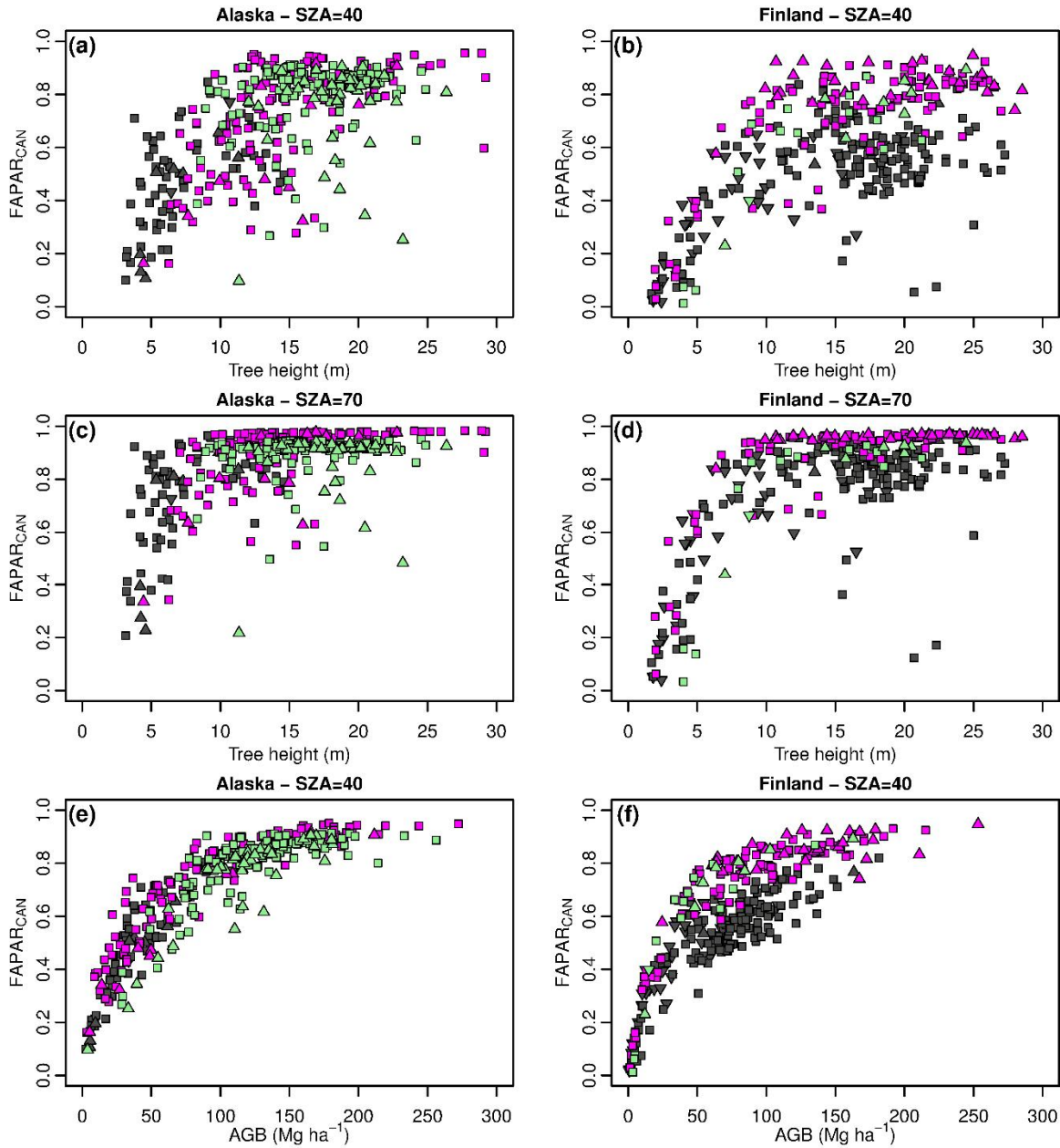
687

688 Figure 3. Spectra of vegetation elements used in the simulations: (a) leaves/shoots, (b) bark, (c) forest floor. The values for  
 689 leaf and shoot are single scattering albedos (reflectance + transmittance), and the values for bark and forest floor are  
 690 reflectance factors.



691

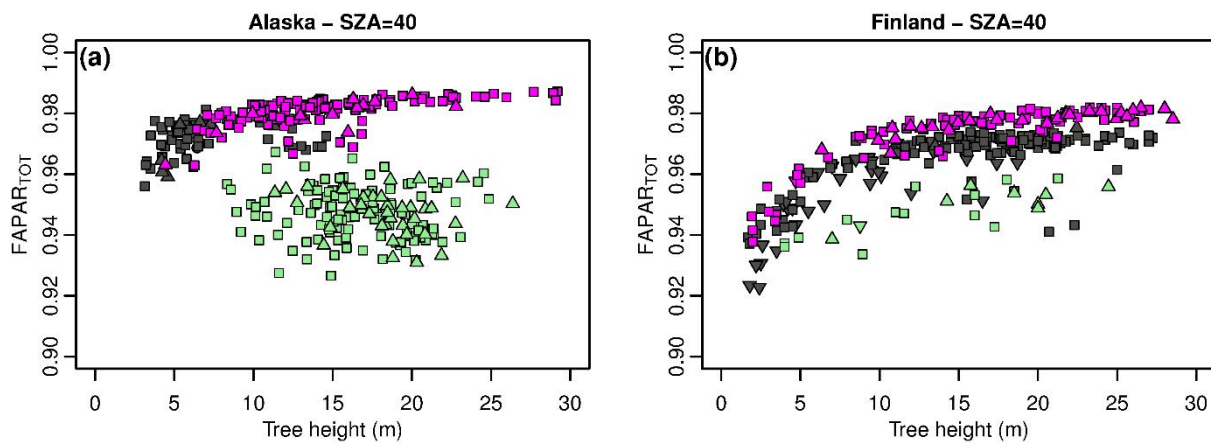
692 Figure 4. Forest black-sky albedo as a function of tree height (a–d) and AGB (e–f). Relations to tree height are shown for  
 693 two SZAs, 40° (a–b) and 70° (c–d), representing solar noon at midsummer and the annual average in the study regions. Left  
 694 hand column shows the results for the Alaskan data, and right hand column for the Finnish data. The figures show only  
 695 monospecific plots, i.e. plots in which the basal area proportion of one of the species exceeded 80%.



696

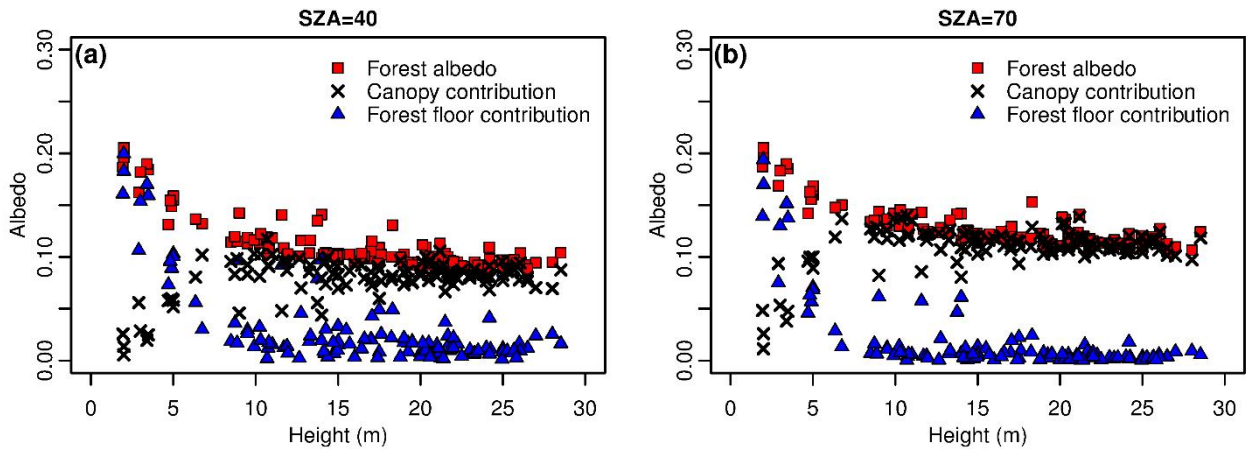
697 Figure 5. Black-sky FAPAR<sub>CAN</sub> as a function of tree height (a–d) and AGB (e–f). Relations to tree height are shown for two  
 698 SZAs, 40° (a–b) and 70° (c–d), representing solar noon at midsummer and the annual average in the study regions. Left hand  
 699 column shows the results for the Alaskan data, and right hand column for the Finnish data. The figures show only  
 700 monospecific plots i.e. plots in which the basal area proportion of one of the species exceeded 80%. For explanation of the  
 701 symbols, see legend in Fig. 4.





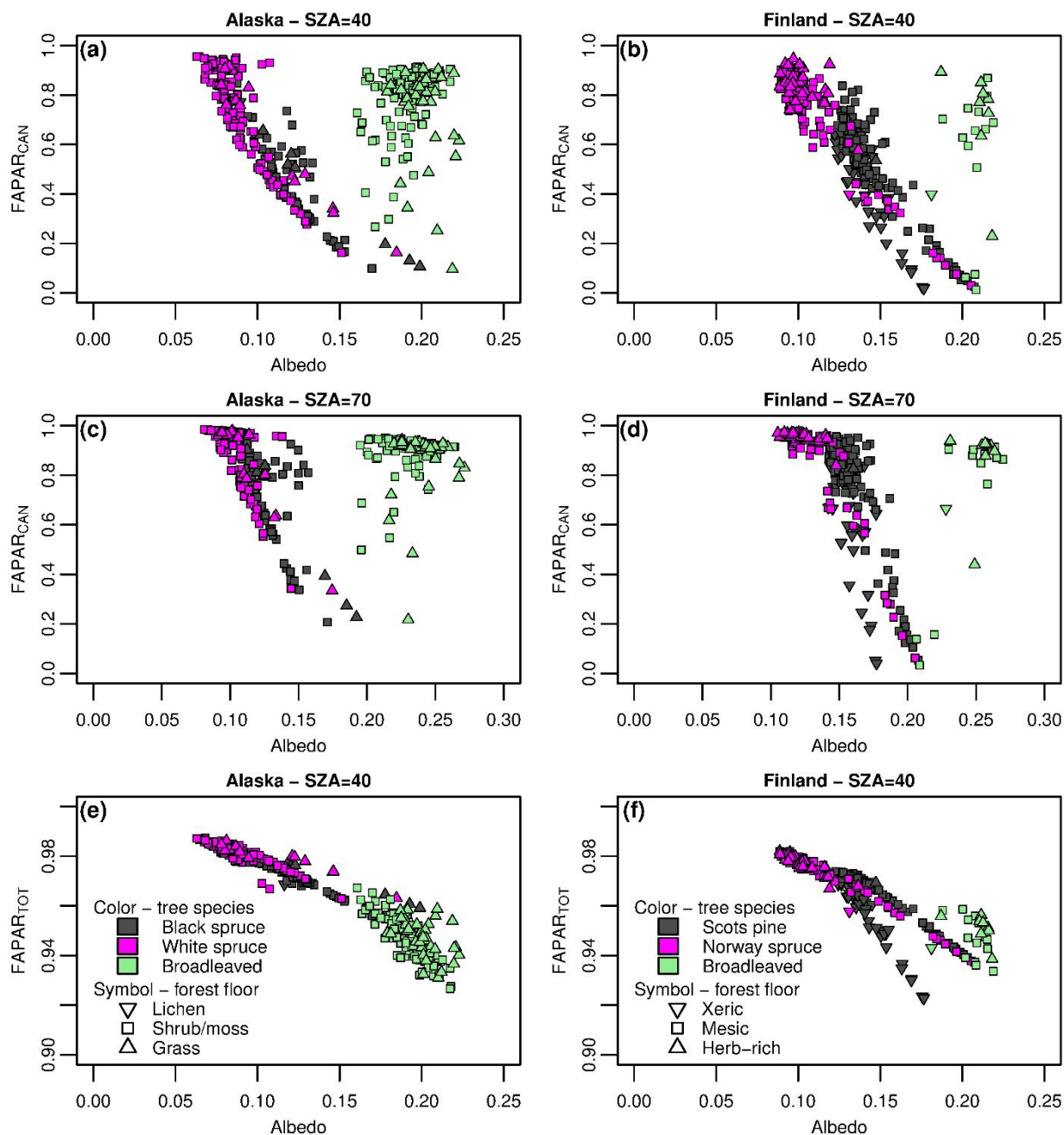
702

703 Figure 6. FAPAR<sub>TOT</sub> as a function of tree height at SZA of 40°. The figures show only monospecific plots i.e. plots in which  
 704 the basal area proportion of one of the species exceeded 80%. For explanation of the symbols, see legend in Fig. 4.



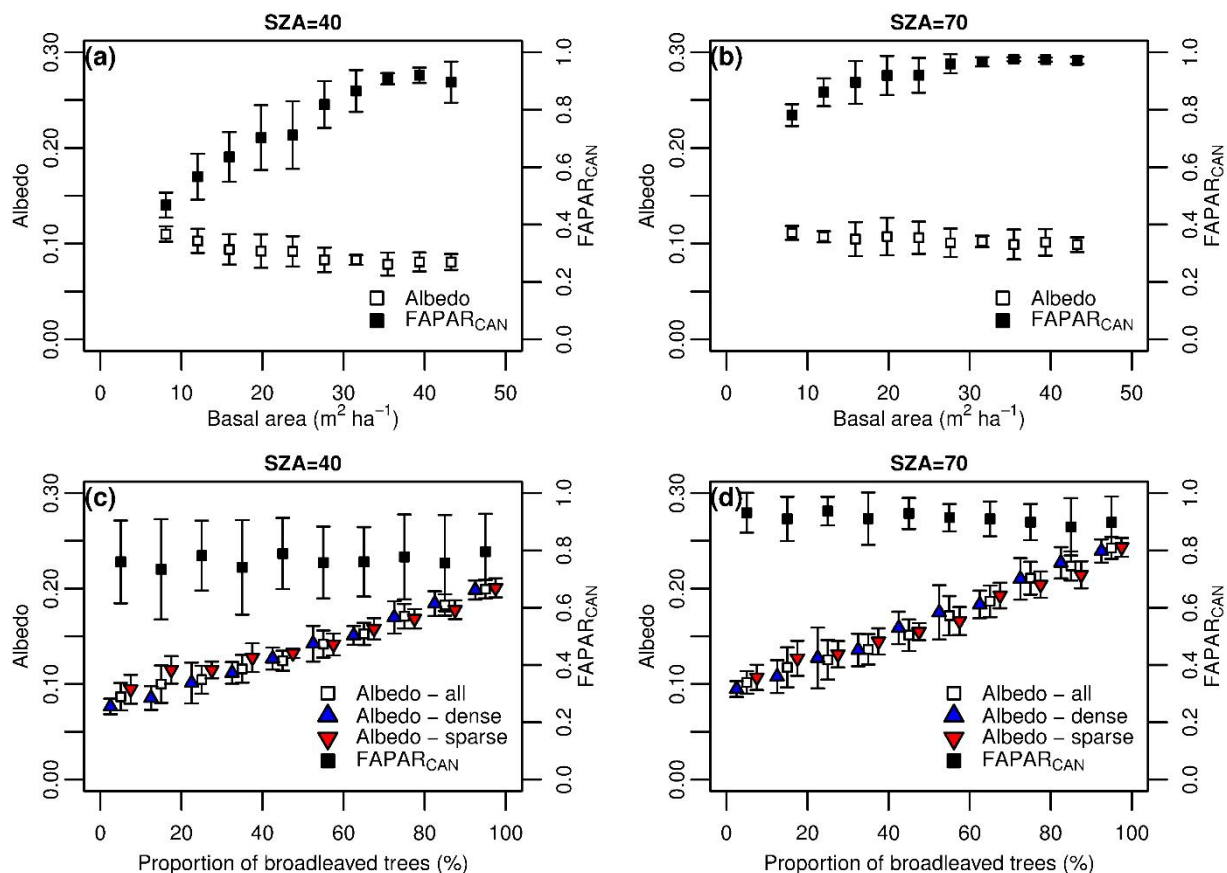
705

706 Figure 7. Canopy and forest floor contributions to forest black-sky albedo as function of tree height. Canopy contribution  
 707 was obtained by assuming black soil in the simulation. Forest floor contribution was obtained by subtracting the canopy  
 708 contribution from the total forest albedo. The data shown are from Norway spruce dominated forests in Finland.



709

710 Figure 8. Relation of FAPAR to forest black-sky albedo by dominant tree species. The figures show only plots that were  
 711 dominated by one species i.e. in which the basal area proportion of one of the species exceeded 80%. a–d: FAPAR<sub>CAN</sub>  
 712 against albedo at two SZAs, 40° and 70°, representing solar noon at midsummer and the annual average in the study regions;  
 713 e–f: FAPAR<sub>TOT</sub> against albedo at SZA of 40°.



714

715 Figure 9. Effect of basal area (a–b) and proportion of broadleaved trees (c–d) on black-sky albedo and FAPAR<sub>CAN</sub> at sun  
 716 zenith angles of 40° and 70° in Alaska. Points represent mean and whiskers the standard deviation in ten equally spaced  
 717 classes. Effect of broadleaved proportion on albedo is presented separately for dense (basal area > 31 m<sup>2</sup> ha<sup>-1</sup>) and sparse  
 718 (basal area < 21 m<sup>2</sup> ha<sup>-1</sup>) forest. These limits correspond to 30th and 70th percentiles of basal area in Alaskan data. The  
 719 points representing dense and sparse forest are shifted along the x axis in order to make them visible.